Ab initio study of Al-ceramic interfacial adhesion

Donald J. Siegel,[1,*,†] Louis G. Hector, Jr.,[2] and James B. Adams[3]
[1]*Department of Physics, University of Illinois at Urbana-Champaign, 1110 West Green Street, Urbana, Illinois 61801*
[2]*Materials and Processes Laboratory, Mail Code 480-106-224, General Motors Research and Development Center, 30500 Mound Road, Warren, Michigan 48090-9055*
[3]*Chemical and Materials Engineering Department, Arizona State University, Tempe, Arizona 85287-6006*
(Received 20 May 2002; published 26 March 2003)

We present a small database of adhesion energies for Al/ceramic interfaces calculated using density functional methods. In total, 26 distinct interface geometries were examined, in which the ceramic component was varied amongst carbides (WC, VC), nitrides (VN, CrN, TiN), and oxides (α-Al_2O_3), while including variations in interfacial stacking sequence and ceramic termination (polar and nonpolar). We find that adhesion is smallest (largest) for those interfaces constructed from non-polar (polar) surfaces, regardless of ceramic component. Since the interfacial free energies of all interfaces are relatively small, we examine the extent to which adhesion can be described solely by contributions from the surface energies.

DOI: 10.1103/PhysRevB.67.092105 PACS number(s): 68.35.−p, 73.20.−r, 71.15.Mb, 71.15.Nc

Interfaces between metals and ceramics play a vital role in many industrial applications:[1] heterogeneous catalysis, microelectronics, thermal barriers, corrosion protection, and metals processing are but a few representative examples. Nonetheless, experimental complications associated with the study of a buried interface, and theoretical difficulties arising from complex interfacial bonding interactions have hindered the development of models capable of predicting fundamental interfacial quantities. Recently, advances in *ab initio* simulation techniques and the development of high resolution experimental probes have made interfacial studies more tractable, as evidenced by the appearance of several papers[2–11] addressing the issue of metal-ceramic adhesion.[1] However, with the exception of only one study,[7] all of these focused on but one or two particular interface systems. These works have provided valuable insight into the atomic and electronic structure of several different interfaces, but the disparity of methods and approximations used (especially in the context of the *ab initio* calculations) can lead to difficulty in comparing results obtained by different groups and consequently inhibit a more fundamental understanding of interfacial properties.

Here we present a small database of adhesion energies for Al/ceramic interfaces compiled both from our earlier reports[12–14] and new calculations on CrN(100), TiN(100), and WC($11\bar{2}0$). We have endeavored to be consistent in our methodology by using a uniform set of calculation parameters for all systems considered. This is significant because earlier studies have, for example, revealed discrepancies between results obtained with different exchange-correlation functionals.[7,12] We have chosen to focus on Al as the metallic component because it is fairly representative of free electron metals, and it receives widespread use in practical applications ranging from microelectronics to structural materials. For ceramics, we have intentionally selected a broad class of compounds [oxides (α-Al_2O_3), carbides (WC, VC), and nitrides (VN, CrN, TiN)], and have examined various interfacial stacking sequences and surface terminations in order to make our survey as general as possible. It is hoped that such a broad sampling would facilitate predictions of interfacial properties through the identification of numerical correlations; for example, based on our results we examine the extent to which adhesion can be attributed to contributions from the surface energies alone. On the other hand, by varying the ceramic component, several of the microscopic properties relevant to interfacial adhesion change simultaneously (crystal structure, surface termination, metalloid atom), thereby complicating an analysis of trends in these underlying quantities. An analysis of these issues—although extremely important—is beyond the scope of this Brief Report, and we refer the reader instead to Refs. 15 and 16.

A fundamental quantity which influences the mechanical properties of an interface is the work of separation $\mathcal{W}_{sep}$(Ref. 1) (also commonly referred to as the "ideal work of adhesion") which is defined as the energy required to break interfacial bonds and reversibly separate the interface into two free surfaces, neglecting diffusion and plastic deformation. (The degree of plastic deformation which occurs during interfacial fracture is known to depend upon $\mathcal{W}_{sep}$.[17]) Formally, $\mathcal{W}_{sep}$ is defined either in terms of the surface and interfacial energies, relative to the respective bulk materials, or by the difference in total energy between the interface and its isolated surfaces

$$\mathcal{W}_{sep}=\sigma_{1v}+\sigma_{2v}-\gamma_{12}=(E_1^{tot}+E_2^{tot}-E_{12}^{tot})/A. \tag{1}$$

Here σ_{iv} is the surface energy of slab i, γ_{12} is the interface energy, E_i^{tot} is the total energy of slab i, and E_{12}^{tot} is the total energy of the interface system. The total interface area is given by A.

Although Eq. (1) defines $\mathcal{W}_{sep}$ in terms of both the surface and interfacial energies, our calculations will illustrate that these quantities do not necessarily play an equal role. We find that since γ is generally small for these metal-ceramic systems, the strength of the interfacial bonding (and thus $\mathcal{W}_{sep}$) depends to a large extent upon the reactivity of the individual surfaces, as reflected by their surface energies. As large σ's indicate the presence of energetically unfavorable features such as large surface dipoles and dangling bonds, these surfaces often reconstruct or seek to passify their dangling bonds by bonding to adsorbates or, when possible, other surfaces. Hence, to first approximation, knowledge of

TABLE I. Comparison of calculated bulk properties with experiment. Experimental data are listed in the second row for each material.

System	a (Å)	c (Å)	B_0 (GPa)	E_{coh} (eV)
Al	4.039		73.5	3.51
	4.03 [a]		79.4 [b]	3.39 [c]
α-Al_2O_3	4.792	13.077	246	33.0
	4.763 [d]	12.98 [d]	253 [e]	31.8 [f]
WC	2.920	2.840	375	16.7
	2.904 [g]	2.835 [g]	443 [g]	16.7 [h]
VN	4.132		316	12.2
	4.126 [i]			12.5 [j]
VC	4.170		304	13.9
	4.172 [i]			13.9 [j]
CrN	4.058		326	10.1
	4.140 [i]			10.3 [j]
TiN	4.253		280	14.2
	4.240 [i]		288 [k]	13.4 [j]

[a]Ref. 26.
[b]Ref. 27.
[c]Ref. 28.
[d]Refs. 29,30.
[e]Ref. 31.
[f]Ref. 32.
[g]Ref. 33.
[h]Ref. 34.
[i]Ref. 35.
[j]Ref. 36.
[k]Ref. 37.

the σ's alone enables one to make a rough prediction of the strength of interfacial bonding and $\mathcal{W}_{sep}$.

For this study we employ density functional theory (DFT),[18,19] as implemented in the Vienna *ab initio* simulation package (VASP).[20] VASP uses a plane-wave basis set for the expansion of the single particle Kohn-Sham wavefunctions, and pseudopotentials[21,22] to describe the computationally expensive electron-ion interaction. Sampling of the irreducible wedge of the Brillouin zone is performed with a Monkhorst-Pack grid of special **k**-points.[23] Ground state atomic geometries for all interfaces and surfaces were obtained by minimizing the Hellman-Feynman forces[24] to a tolerance of 0.05 eV/Å per atom. All calculations employed the generalized gradient approximation (GGA) of Perdew and Wang.[25]

To ensure the precision of energies and geometries, **k**-point and planewave cutoff energy convergence tests were performed, resulting in total energies which were converged to within 1–2 meV per atom. The accuracy of the pseudopotential approximation was assessed by performing calculations on the bulk phases of all materials used in this study. The results of these calculations are compiled in Table I and compared with available experimental data; consistent with other GGA-DFT studies, we find excellent agreement. More detailed accounts of the pseudopotential implementations and convergence testing can be found elsewhere.[12–14]

As our goal was to simulate surfaces and interfaces of bulklike materials, additional checks were performed to ensure that the slabs comprising each interface were sufficiently thick to exhibit a bulklike interior. In order to accurately evaluate surface energies (see Table II) we followed the method proposed by Boettger,[38] which avoids the problem of non-convergence of σ with respect to slab thickness. Large slabs of up to 15 atomic layers were used. For the polar surfaces, α-$Al_2O_3(0001)^O$, $WC(0001)^W$, and $WC(0001)^C$ (superscripts indicate the termination), a nonstoichiometric slab must be implemented to allow for identical termination of both surfaces. In those cases it is only possible to calculate the surface energy within a range where the chemical potentials of the elements in the compound μ_i are less than those of the pure elements in their standard states (SS): $\mu_i \leqslant \mu_i^{SS}$ (see our earlier paper[13] or Refs. 39,40 for more details). The average of σ over this range is reported in Table II and was then used in relating $\mathcal{W}_{sep}$ to σ. We note that of the 12 σ's reported in that table, three of the four largest belong to polar surfaces, in which cleaving the surface requires the breaking of strong anion-cation bonds. (All of the ceramics exhibit some degree of ionic/polar-covalent bonding.) The remaining eight nonpolar surfaces have smaller surface energies $\sigma \leqslant 1.6\ \mathrm{J\,m^{-2}}$.

TABLE II. Calculated surface energies σ and slab dimensions (given in No. of atomic layers) used in the interface calculations. For the nonstoichiometric slabs both the average σ and the range of possible σ are given. Superscripts give the termination of those surfaces cleaved along a polar plane.

Surface	No. Layers	σ (J m^{-2})
Al(100)	5	0.89
Al(110)	4	1.05
Al(111)	5	0.81
α-$Al_2O_3(0001)^{Al}$	15	1.59
α-$Al_2O_3(0001)^{O}$	13	7.64, (4.45–10.83)
$WC(0001)^W$	9	3.66, (3.43–3.88)
$WC(0001)^C$	9	5.92, (5.69–6.14)
$WC(11\bar{2}0)$	4	3.88
VN(100)	7	0.95
VC(100)	7	1.28
CrN(100)	7	0.74
TiN(100)	7	1.25

Due to the substantial computational cost of performing a DFT calculation on supercells containing first row and transition metal elements, we emphasize that our molecular statics (0 K) predictions of structure and $\mathcal{W}_{sep}$ do not account for temperature and larger-scale size effects such as reconstructions and lattice mismatch. Since strain effects can impact $\mathcal{W}_{sep}$,[9] we intentionally selected ceramics having a mismatch with the Al lattice of roughly less than 5% (see Table III). A realistic interface with a mismatch of this magnitude would likely possess large regions of coherency interrupted by widely spaced ($\gtrsim$100 Å) misfit dislocations; hence our coherent models are reasonable first approximations to the true structures. Even though many transition metal carbides and nitrides generally contain (10–20 %) vacancies at the metalloid sites,[41] our models use ideal 1:1 stoichiometries to allow the use of smaller supercells.[46]

Our interface models used a superlattice geometry in which a central ceramic slab was sandwiched between two slabs of Al, resulting in two identical interfaces per supercell. When possible, orientation relationships from experiment[42] were used (see Table III for a complete listing). A vacuum region of $\sim$10 Å separated the free surfaces of the Al. To accommodate the periodic boundary conditions, all but one interface system[47] used the coherent interface approximation in which the lateral dimensions of the softer Al slabs were adjusted to match the surface lattice constants of the ceramic.

For each interface system several different stacking se-

TABLE III. Interfacial orientation relationship, polarity (P = polar, NP = nonpolar), strain, interfacial free energy (γ), and $\mathcal{W}_{sep}$. The terminations of the polar ceramic surfaces are indicated with a superscript. $\mathcal{W}_{sep}$ values correspond to the optimal stacking sequences.

Interface	Orientation	Polarity	Strain (%)	γ (J m^{-2})	$\mathcal{W}_{sep}$ (J m^{-2})
$Al/\alpha\text{-}Al_2O_3{}^{Al}$	$(111)[\bar{1}10]_{Al}\|\|(0001)[10\bar{1}0]_{Al_2O_3}$	NP	4.9	1.34	1.06
$Al/\alpha\text{-}Al_2O_3{}^{O}$	$(111)[\bar{1}10]_{Al}\|\|(0001)[10\bar{1}0]_{Al_2O_3}$	P	4.9	-1.28	9.73
Al/WC^{W}	$(111)[\bar{1}10]_{Al}\|\|(0001)[11\bar{2}0]_{WC}$	P	2.2	0.39	4.08
Al/WC^{C}	$(111)[\bar{1}10]_{Al}\|\|(000\bar{1})[11\bar{2}0]_{WC}$	P	2.2	0.72	6.01
Al/WC	$(110)[1\bar{1}0]_{Al}\|\|(11\bar{2}0)[0001]_{WC}$	NP	0.4	1.79	3.14
Al/VN	$(100)[001]_{Al}\|\|(100)[001]_{VN}$	NP	2.3	0.11	1.73
Al/VC	$(100)[001]_{Al}\|\|(100)[001]_{VC}$	NP	3.2	0.03	2.14
Al/CrN	$(100)[001]_{Al}\|\|(100)[001]_{CrN}$	NP	0.5	0.18	1.45
Al/TiN	$(100)[001]_{Al}\|\|(100)[001]_{TiN}$	NP	5.3	0.62	1.52

quences (i.e., relative translations of the slabs within the plane of the interface) were examined to identify the optimal bonding site. We also considered multiple terminations for the α-Al_2O_3 and WC surfaces: Al and O terminations for α-$Al_2O_3(0001)$ and W and C terminations for WC(0001).

The results of our $\mathcal{W}_{sep}$ calculations are presented in Table III, where one can see that there are substantial differences in $\mathcal{W}_{sep}$ for the polar vs non-polar geometries. In particular, the three polar surfaces have the largest $\mathcal{W}_{sep}$, ranging from 4.08 J m^{-2} for Al/WC^{W} up to 9.73 J m^{-2} for $Al/\alpha\text{-}Al_2O_3{}^{O}$. Of the remaining six (nonpolar) interfaces, five have $\mathcal{W}_{sep}$ values of 2.1 J m^{-2} or less. The $\mathcal{W}_{sep}$'s for the three nitride ceramics are among the smallest overall, and are relatively insensitive to the choice of metallic component, with $\mathcal{W}_{sep}$ falling within 1.45–1.73 J m^{-2}. On average, the polar $\mathcal{W}_{sep}$'s are 4.6 J m^{-2} larger than the non-polar systems, consistent with their larger surface energies. We note that our predicted $\mathcal{W}_{sep}$ value of 1.06 J m^{-2} for $Al/\alpha\text{-}Al_2O_3{}^{Al}$ compares favorably with the experimental[43] (sessile drop) value of 1.13 J m^{-2} as scaled to 0 K. To our knowledge, experimental adhesion data for the other interface systems is unavailable.

Regarding the optimal interfacial stacking sequences, we find that for the Al/α-Al_2O_3 and polar Al/WC systems the metal atoms prefer sites which continue the natural stacking sequence of the bulk ceramic across the interface and into the Al. For Al/VC, Al/VN, Al/CrN, Al/TiN, and Al/WC$(11\bar{2}0)$, the Al atoms prefer to sit above the metalloid atoms (C and N). More details regarding some of the individual interfaces, including an analysis of interfacial electronic structure, can be found in Refs. 12–14.

Table III also lists the interfacial energies, and shows that they are relatively small (on average ~19%) in comparison to the summed surface energies, $\sigma_{Al}+\sigma_{ceramic}$ (Table II). The generally small magnitude of γ suggests that the σ's are the dominant term in Eq. (1) for these metal-ceramic systems. To further examine the extent to which $\mathcal{W}_{sep}$ can be determined by the surface energies alone, Fig. 1 plots $\mathcal{W}_{sep}$ vs $\sigma_{Al}+\sigma_{ceramic}$; a line with unit slope is also included to indicate where the data points would lie in the idealized case of $\gamma=0$. In this representation the horizontal deviation of a given data point from the $\gamma=0$-line corresponds to the size of γ. For the three polar interfaces at the top of the figure, the data are bracketed by horizontal error bars giving the range of possible σ listed in Table II. While the $\mathcal{W}_{sep}$ data on the whole follow a roughly linear trend with respect to σ, all but one of the data points fall to the right of the line. This reveals that bonding at these interfaces is on average weaker than in the respective bulk regions. The one system falling to the left of the line, and therefore having a negative γ, involves the oxygen-terminated α-Al_2O_3 surface, which has the largest surface energy and $\mathcal{W}_{sep}$. In an earlier paper[12] we argued that the strong bonding at this interface could indicate the possibility of fracture within the Al rather than at the metal-ceramic junction, were the interface subjected to a tensile stress.

With the exception of TiN, the rocksalt-structured carbides and nitrides (CrN, VN, and VC) exhibit the largest dependence of $\mathcal{W}_{sep}$ upon the surface energies. These three systems have the smallest interfacial energies, only 0.03–0.18 J m^{-2}, and their $\mathcal{W}_{sep}$'s cluster in a nearly linear fashion along the bottom left of Fig. 1, close to the $\gamma=0$ line. Presumably, the smallness of γ for these interfaces can be explained by similarities between bulk and interfacial bonding, since both bulk components exhibit some degree of metallic bonding. We note that two earlier studies[44,45] involving (Al/Ag/Ti)/MgO observed a similar dependence of $\mathcal{W}_{sep}$ upon metallic surface energies. For Al/TiN, which is some-

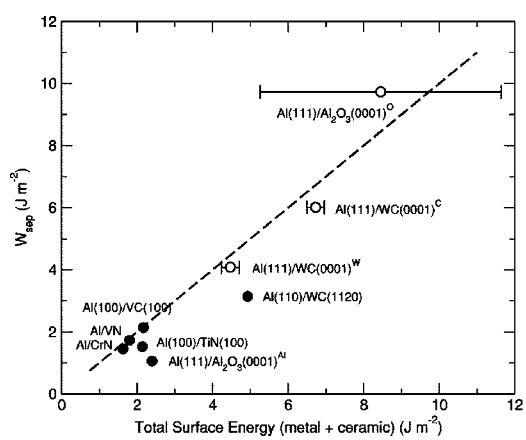

FIG. 1. $\mathcal{W}_{sep}$ vs the summed surface energies ($\sigma_{Al}+\sigma_{ceramic}$). Filled (open) circles correspond to nonpolar (polar) interfaces. The dotted line corresponds to the case $\gamma=0$.

what of an outlyer with respect to the other rocksalt ceramics, the γ contribution is larger, 0.62 J m^{-2}, possibly due to the relatively large interfacial strain of 5.3%.

Figure 1 also illustrates that those interfaces involving α-Al_2O_3 and WC($11\overline{2}0$) have $\mathcal{W}_{sep}$'s which are not as well described by surface energies alone (i.e., γ effects are more important). For the α-Al_2O_3 interfaces, as with TiN, a possible explanation for this behavior could be strain effects, which are also significant (4.9%) for this system. In addition, the mainly ionic bonding in bulk α-Al_2O_3 differs substantially from that found in Al. While for the WC system the strain is low (0.4%), and differences in the respective bulk bonding are less pronounced (WC is metallic), this model implements an incoherent, misfit geometry characterized by irregular bonding across the interface.

In summary, we have presented a small *ab initio* database of adhesion energies for nine Al/ceramic interfaces, surveying several different interface terminations and bonding sites. We show that the surface energies play a dominant role in determining the work of separation for these systems, as the interfacial energies are generally much smaller in comparison. In most cases, and in particular for those systems involving the cubic carbides and nitrides, $\mathcal{W}_{sep}$ can be described largely in terms of surface energies alone. Exceptions to this rule arise mainly for systems characterized by relatively large interfacial strain or incoherent interfacial bonding. Knowledge of the surface energies could therefore serve as a reasonable starting point for the estimation of interfacial strength.

Computational resources for this study were provided by the National Computational Science Alliance at the University of Illinois at Urbana-Champaign under Grant No. MCA 96N001N. Financial support was provided by the National Science Foundation Division of Materials Research under grant DMR 9619353.

*Email address: djsiege@sandia.gov

†Current address: Sandia National Laboratories, Mail Stop 9161, Livermore, CA 94551.

[1] M. W. Finnis, J. Phys.: Condens. Matter **8**, 5811 (1996).

[2] J. R. Smith, T. Hong, and D. J. Srolovitz, Phys. Rev. Lett. **72**, 4021 (1994).

[3] G. Song *et al.*, Phys. Rev. Lett. **79**, 5062 (1997).

[4] D. A. Muller *et al.*, Phys. Rev. Lett. **80**, 4741 (1998).

[5] C. Verdozzi *et al.*, Phys. Rev. Lett. **82**, 799 (1999).

[6] I. G. Batirev *et al.*, Phys. Rev. Lett. **82**, 1510 (1999).

[7] A. Bogicevic and D. R. Jennison, Phys. Rev. Lett. **82**, 4050 (1999).

[8] Y. F. Zhukovskii *et al.*, Phys. Rev. Lett. **84**, 1256 (2000).

[9] R. Benedek *et al.*, Phys. Rev. Lett. **84**, 3362 (2000).

[10] S. V. Dudiy, J. Hartford, and B. I. Lundqvist, Phys. Rev. Lett. **85**, 1898 (2000).

[11] W. Zhang and J. R. Smith, Phys. Rev. Lett. **85**, 3225 (2000).

[12] D. J. Siegel, L. G. Hector, Jr., and J. B. Adams, Phys. Rev. B **65**, 085415 (2002).

[13] D. J. Siegel, L. G. Hector, Jr., and J. B. Adams, Surf. Sci. **498**, 321 (2002).

[14] D. J. Siegel, L. G. Hector, Jr., and J. B. Adams, Acta Mater. **50**, 619 (2002).

[15] A. M. Stoneham, M. M. D. Ramos, and A. P. Sutton, Philos. Mag. A **67**, 797 (1993).

[16] J.-G. Li, Ceram. Trans. **35**, 81 (1995).

[17] D. M. Lipkin, D. R. Clarke, and A. G. Evans, Acta Mater. **46**, 4835 (1998).

[18] P. Hohenberg and W. Kohn, Phys. Rev. **136**, B864 (1964).

[19] W. Kohn and L. J. Sham, Phys. Rev. **140**, A1133 (1965).

[20] G. Kresse and J. Furthmüller, Phys. Rev. B **54**, 11 169 (1996).

[21] D. Vanderbilt, Phys. Rev. B **41**, 7892 (1990).

[22] G. Kresse and J. Hafner, J. Phys.: Condens. Matter **6**, 8245 (1994).

[23] H. J. Monkhorst and J. D. Pack, Phys. Rev. B **13**, 5188 (1976).

[24] R. P. Feynman, Phys. Rev. **56**, 340 (1939).

[25] J. P. Perdew *et al.*, Phys. Rev. B **46**, 6671 (1992).

[26] *Thermophysical Properties of Matter*, edited by Y. S. Touloukian *et al.* (Plenum, New York, 1975), Vol. 12.

[27] G. Simmons and H. Wang, *Single Crystal Elastic Constants and Calculated Aggregate Properties: A Handbook*, 2nd ed. (MIT Press, Cambridge, MA, 1971).

[28] C. Kittel, *Introduction to Solid State Physics*, 6th ed. (John Wiley and Sons, New York, 1986).

[29] *Thermophysical Properties of Matter*, edited by Y. S. Touloukian *et al.* (Plenum, New York, 1977), Vol. 13.

[30] L. W. Finger and R. M. Hazen, J. Appl. Phys. **49**, 5823 (1978).

[31] P. Richet, J. Xu, and H. K. Mao, Phys. Chem. Miner. **16**, 207 (1988).

[32] *CRC Handbook of Chemistry and Physics*, edited by R. C. Weast (CRC Press, Boca Raton, FL, 1983), 67th ed.

[33] R. Reeber and K. Wang, J. Am. Ceram. Soc. **82**, 129 (1999).

[34] A. Y. Liu, R. M. Wentzcovitch, and M. L. Cohen, Phys. Rev. B **38**, 9483 (1988).

[35] *Pearson's Handbook of Crystallographic Data for Intermetallic Phases*, edited by P. Villars and L. D. Calvert (ASM International, Materials Park, OH, 1991), Vols. 2,4.

[36] J. Häglund *et al.*, Phys. Rev. B **43**, 14 400 (1991).

[37] A. G. Milevskii *et al.*, Phys. Status Solidi B **198**, 629 (1996).

[38] J. C. Boettger, Phys. Rev. B **49**, 16 798 (1994).

[39] K. Rapcewicz *et al.*, Phys. Rev. B **57**, 7281 (1998).

[40] X.-G. Wang *et al.*, Phys. Rev. Lett. **81**, 1038 (1998).

[41] L. E. Toth, *Transition Metal Carbides and Nitrides* (Academic Press, New York, 1971).

[42] D. L. Medlin, K. F. McCarthy, R. Q. Hwang, S. E. Guthrie, and M. I. Baskes, Thin Solid Films **299**, 110 (1997).

[43] D. M. Lipkin, J. N. Israelachvili, and D. R. Clarke, Philos. Mag. A **76**, 715 (1997).

[44] T. Hong, J. R. Smith, and D. J. Srolovitz, Acta Metall. Mater. **43**, 2721 (1995).

[45] U. Schönberger, O. K. Andersen, and M. Methfessel, Acta Metall. Mater. **40**, S1 (1992).

[46] We take CrN to be in its room-temperature paramagnetic state.

[47] The Al/WC($11\overline{2}0$) system contains a misfit: a (4×1) surface of WC($11\overline{2}0$) is interfaced to a (5×1) Al(110). The large supercell needed for this calculation made a superlattice geometry impractical, and the interface was formed at only one surface of the WC.